Vibration-Based Support Vector Machine for Structural Health Monitoring

Conference Paper · July 2017

DOI: 10.1007/978-3-319-67443-8_14

5 authors, including:

Hong Pan
Tongji University
35 PUBLICATIONS **728** CITATIONS
SEE PROFILE

Mohsen Azimi
University of British Columbia
33 PUBLICATIONS **912** CITATIONS
SEE PROFILE

Fei Yan
North Dakota State University
21 PUBLICATIONS **914** CITATIONS
SEE PROFILE

Zhibin Lin
North Dakota State University
116 PUBLICATIONS **2,321** CITATIONS
SEE PROFILE

Vibration-Based Support Vector Machine for Structural Health Monitoring

Hong Pan[1,2,3], Mohsen Azimi[3], Guoqing Gui[1], Fei Yan[3], and Zhibin Lin[3(✉)]

[1] School of Architecture and Civil Engineering, Jinggangshan University, Ji'an 343009, Jiangxi, China
[2] College of Civil Engineering, Tongji University, 1239 Siping Road, Shanghai, China
[3] Department of Civil and Environmental Engineering, North Dakota State University, Fargo, ND, USA
zhibin.lin@ndsu.edu

Abstract. There are ever-increasing interests to determine effectively structural diagnosis and conditional assessment for structural health monitoring (SHM). Although research has been extensively conducted in the conventional physical-based vibration analysis, advancement in sensor technologies and complexity in structural systems post great challenges in the effectiveness of these techniques. Alternatively, various data-driven based machine learning techniques are recently emerging tools to data clarification. In this study, a new vibration-based machine learning was proposed for condition assessment and damage detection in SHM. Three vibration-based feature extraction methods, autoregressive, vector autoregressive and singular value decomposition methods, were used as damage sensitive features. A kernel function based support vector machine was used to facilitate the identification between damaged and undamaged cases. A benchmark with varying environment and operational conditions in the literature was selected to verify the effectiveness of the proposed methods. The results showed that three feature methods could effectively map damage features in a high dimensional feature space, thereby dramatically improving the effectiveness and accuracy of data classification. Moreover, comparisons of results revealed that the singular value decomposition methods exhibit higher sensitivity to damage states as compared to other two approaches.

Keywords: Vibration · Machine learning · Damage feature extraction · Structural health monitoring · Damage detection

1 Introduction

The success of structural health monitoring (SHM) requires techniques that could effectively diagnose the structural conditions and identify any damages/defects experienced in many engineering fields, including aerospace, civil and mechanical engineering. Dynamic responses of structural systems collected by various sensors are usually used as the basis for structural diagnosis in the physical-based analytical models and simulation techniques [1–7]. Advanced development of sensor technologies not

J.P. Conte et al. (eds.), *Experimental Vibration Analysis for Civil Structures*,
Lecture Notes in Civil Engineering 5, https://doi.org/10.1007/978-3-319-67443-8_14

only allows big progress in these methods, but also posts big challenges when facing ever-increasingly complex systems or different interferences.

Data-driven machine learning attracts high interest in large-scale structural systems [8–14]. The key of these data-driven methods for structural diagnosis is to select proper damage features. Although some attentions have been paid to vibration-based feature extraction methods, such as autoregressive model or singular value decomposition methods, it is still a big challenge to assess methods that could better serve as sensitive features. From a systematical standpoint, few attempts are made to address data-driven structural diagnosis and damage detection in terms of applicability of feature extraction techniques. As a result, findings from these previous studies may not fully account for data process. Thus, integration of these new methods in structural diagnosis is necessary to large-scale structural systems.

Therefore, this study aims to develop a data-driven framework for structural diagnosis and damage detection using support vector machine integrated with enhanced feature extraction techniques. Three feature extraction methods were selected. A benchmark was used to calibrate the developed concept and demonstrate the effectiveness and sensitivity of the data-driven damage detection in the SHM.

2 Data-Driven Approaches for Structural Diagnosis in SHM

Data-driven machine learning methods [12] are the statistical strategy for implementing data mining process, as schematically shown in Fig. 1. The data-driven approaches for structural diagnosis in SHM could mainly include four stages: (a) data acquisition and preprocessing of collected sensor data; (b) feature extraction; (c) support vector machine learning for data training and model development for data classification; and (d) conditional assessment and decision making, as shows in the following flow chart in Fig. 1.

The success of the structural diagnosis in SHM is highly dependent of potential sensitive features, such as damages/defects/abnormality. Three vibration-based feature extraction approaches, autoregressive, vector autoregressive and singular value decomposition methods, are selected herein as damage sensitive features and addressed below.

2.1 Features Extraction and Supervised Machine Learning

Feature extraction is crucial to identify potential sensitive features for structural diagnosis. The three different extraction approaches herein are presented to compress and extract the data for potential damage-sensitive features [15].

2.2 Autoregressive Model (AR)

The AR model [15–17] is the time-series based analysis using the linear combination with p parameters:

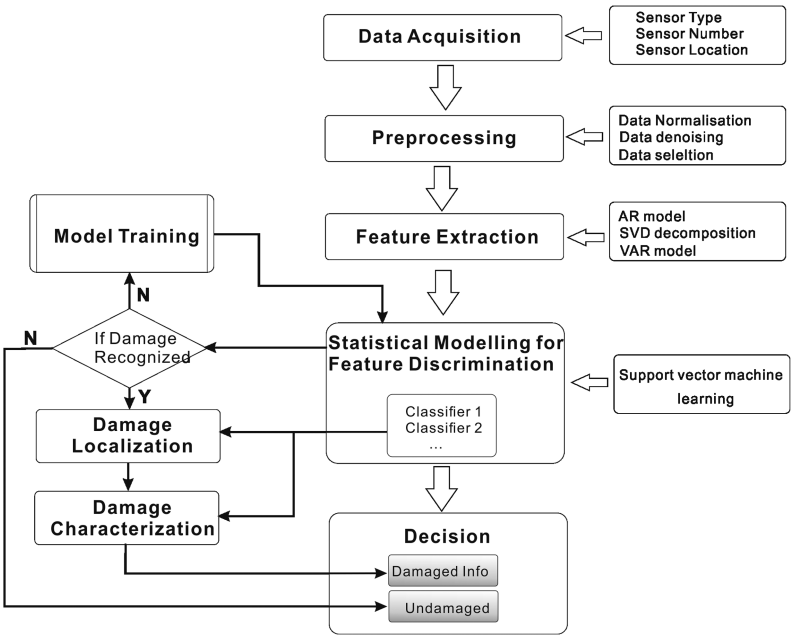

Fig. 1. Flow chart of data-driven approach for SHM.

$$x_i = \sum_{j=1}^{p} \phi_j x(i-j) + e_i \tag{1}$$

where x_i denotes the discrete signal, i denotes the time step, and e_i denotes an error. ϕ_j is unknown AR parameters. The order of the AR model is determined by the Akaike information criterion (*AIC*) method [18]:

$$AIC(p) = N \cdot \ln\sigma_p^2 + 2p \tag{2}$$

where, N is the samples number; and σ_p^2 is the prediction variance of p order model. In [12], the order of AR models ($p = 15$) is sufficient for the convergence.

2.3 Multivariate Vector Autoregressive Model (VAR)

The VAR model is a powerful model to use for multivariate time series [19]. The VAR (p) model can be written as:

$$y_t = a_0 + \sum_{j=1}^{p} A_j y_{t-j} + \varepsilon_t, \tag{3}$$

where y_t is an $M \times 1$ vector on M data acquisition sensor, y_t for $t = 1, \ldots, T$, ε_t is an $M \times 1$ vector of errors which coming from the zero-mean Gaussian distribution with covariance parameter Σ. A_j is an $M \times M$ matrix a_0 is an $M \times 1$ intercepts vector.

The matrix form of VAR model can be written as:

$$\boldsymbol{Y} = \boldsymbol{XA} + \boldsymbol{E}, \tag{4}$$

where $\boldsymbol{Y}$ is a $T \times M$ matrix which stacks the T times of observations data; $\boldsymbol{A}$ is a $(1 + Mp) \times M$ matrix and defined by $\boldsymbol{A} = \left(a_0 A_1 \ldots A_p\right)'$; and $\boldsymbol{X}$ is a $T \times (1 + Mp)$ matrix. The vector form of Eq. (4) could be rewritten by

$$\boldsymbol{Y} = (\boldsymbol{I} \otimes \boldsymbol{X})\hat{\boldsymbol{\alpha}} + \boldsymbol{\varepsilon} \tag{5}$$

where $\hat{\boldsymbol{\alpha}} = vec\left(\hat{\boldsymbol{A}}\right)$ and $\hat{\boldsymbol{A}} = \left(\boldsymbol{X}'\boldsymbol{X}\right)^{-1}\boldsymbol{X}'\boldsymbol{Y}$ are determined by the ordinary least squares estimation. Vector $\hat{\boldsymbol{\alpha}}$ is to define a relation between the own lag and different variable lag and has been reported as the damage sensitive feature. It is different from AR model, as they have different variable lag coefficients.

2.4 Singular Value Decomposition (SVD)

The singular value decomposition is a mathematical method [14], which seeks an orthogonal basis for representation of the linear data space. Assume $\boldsymbol{X}$ is a $M \times N$ matrix. The relationship between the rank of a matrix and the independent hidden variables of the data is closed. In the context of the SVD, it is possible to find the approximate data by using some main hidden variables. Hence, the SVD can be seen as a linear method to separate the main signal and noise from others. The decomposition of the matrix $\boldsymbol{X}$ can be express as:

$$\boldsymbol{X} = \boldsymbol{U\Sigma V}' = \sum\nolimits_{i=1}^{\gamma} \sigma_i \mu_i \upsilon_i' \tag{6}$$

where the $\boldsymbol{U}$ and $\boldsymbol{V}$ are the orthonormal matrix with a dimension of $M \times M$ and $N \times N$;

$$\boldsymbol{U} = [\boldsymbol{\mu}_1 \boldsymbol{\mu}_2 \ldots \boldsymbol{\mu}_m], \boldsymbol{V} = [\upsilon_1 \upsilon_2 \ldots \boldsymbol{\upsilon}_n], \boldsymbol{U}'\boldsymbol{U} = \boldsymbol{I}_{\mathrm{m}} \text{ and } \boldsymbol{V}'\boldsymbol{V} = \boldsymbol{I}_{\mathrm{n}} \tag{7}$$

and the $\boldsymbol{\Sigma}$ is a $M \times N$ diagonal matrix and the signaler nonzero diagonal values of the matrix $\boldsymbol{\Sigma}$ are arranged by

$$\sigma_1 \geq \sigma_2 \geq \cdots \geq \sigma_\gamma = \cdots = \sigma_{min} = 0 \tag{8}$$

It is common to assume that, $\gamma \leq \mathrm{N}$, that it is, the number of data space variables is bigger than the number of independent data variables. The vectors $\mu_i(\upsilon_i)$ adjacent to the i_{th} singular value σ_i can span an orthonormal n-dimensional space $\mathbb{R}^n$.

$$\boldsymbol{X} = \boldsymbol{U\Sigma V}' = \begin{bmatrix} \boldsymbol{U}_\Upsilon & \boldsymbol{U}_\Upsilon^\perp \end{bmatrix} \begin{bmatrix} \boldsymbol{\Sigma}_\gamma & 0 \\ 0 & 0 \end{bmatrix} \begin{bmatrix} \boldsymbol{V}_\gamma' \\ \left(\boldsymbol{V}_\gamma^\perp\right)^H \end{bmatrix} \tag{9}$$

where

$$\boldsymbol{U}_{\gamma} = \left[\boldsymbol{\mu}_1 \boldsymbol{\mu}_2 \ldots \boldsymbol{\mu}_{\gamma}\right], \text{ and } \boldsymbol{U}_{\gamma}^{\perp} = \left[\boldsymbol{\mu}_{\gamma+1} \boldsymbol{\mu}_{r+2} \ldots \boldsymbol{\mu}_m\right] \tag{10a}$$

$$\boldsymbol{V}_r = \left[\boldsymbol{\upsilon}_1 \boldsymbol{\upsilon}_2 \ldots \boldsymbol{\upsilon}_{\gamma}\right], \text{ and } \boldsymbol{V}_{\gamma}^{\perp} = \left[\boldsymbol{\upsilon}_{\gamma+1} \boldsymbol{\upsilon}_{\gamma+2} \ldots \boldsymbol{\upsilon}_n\right] \tag{10b}$$

$$\boldsymbol{\Sigma}_{\gamma} = diag(\sigma_1, \ldots, \sigma_{\gamma}) \tag{10c}$$

The singular vector μ_i or υ_i are treated as the dominant singular vectors. For signal $\boldsymbol{X}$, the number of dominant orthonormal dimensional can be selected based on the Forbenius-norms as:

$$\|\boldsymbol{X}\|_F = \sqrt{\sum_{i=1}^{n} \sum_{j=1}^{m} \left|x_{ij}\right|^2} = \left\|\boldsymbol{U}\boldsymbol{\Sigma}\boldsymbol{V}'\right\|_F = \|\boldsymbol{\Sigma}\|_F = \sqrt{\left(\sigma_1^2 + \ldots + \sigma_n^2\right)} \tag{11}$$

The energy of the data is preserved in the singular value spectrum σ_i [14]. For noise-corrupted signals the denoising process can be treat like a delete of some minima σ_i. In general decomposition process, one needs reshape the signal to a Hankel matrix, and then uses SVD to decompose the Hankel matrix, determine the number p of singular value spectrum σ_i selected and finally generate the denoised signal and noise:

$$\boldsymbol{X} = \boldsymbol{X}_0 + \boldsymbol{X}_{noise} \tag{12}$$

where $\boldsymbol{X}_0$ is the first raw of $\boldsymbol{H}_{X_0}$. $\boldsymbol{X}_{noise}$ is the residual of the denoised signal. The statistical residual of the signal $\boldsymbol{X}$ is also selected as a damage feature vector, as addressed in the following section.

2.5 Three Feature Extraction Techniques and Their Residual Errors

The residual error (RE) has been found as high sensitivity as statistical damage features [12, 21–23]. In this study, the REs for the three feature extraction techniques, AR, SVD and VAR models, are also computed:

$$e_i = x_i - \hat{x}_i \tag{13}$$

where $\hat{x}_i$ is the predicted signal value and the measured signal x_i. A total of sixteen statistical features from the residual errors were summarized from the literature [12, 21–23], as listed in Table 1.

2.6 Supervised Machine Learning Using Support Vector Machine

The SVM, as one of supervised machine learning techniques, is herein used for data classification [12, 24]. By applying Gaussian radial basis function Kernel function, the SVM is defined by the variable ξ_i and the error penalty C:

$$\min\left(\frac{1}{2}\left\|w^2\right\| + C\sum\nolimits_{i=1}^{N}\xi_i\right) \tag{15a}$$

$$\text{subject to } y_{i(w.X)} + b \geq 1 - \xi_i, \xi_i \geq 0 \tag{15b}$$

where w and b refer to the vector and scalar to define the position of the hyperplane. ξ_i denotes a distance measured between the hyperplane.

Table 1. Definition of statistical features [12]

Feature	Formulations	Feature	Formulations
Maximum	$RE_1 = \max(e_i)$	RMS	$RE_9 = rms = \sqrt{\frac{1}{N}\sum_{j=1}^{N} e_i^2}$
Minimum	$RE_2 = \min(e_i)$	Form factor	$RE_{10} = \frac{rms}{\frac{1}{N}\sum_{j=1}^{N}\lvert e_i\rvert}$
Mean	$RE_3 = \mu = \frac{1}{N}\sum_{j=1}^{N} e_i$	Crest factor	$RE_{11} = \frac{\max(e_i)-\min(e_i)}{rms}$
Maximum-minimum	$RE_4 = \max(e_i) - \min(e_i)$	kurtosis factor	$RE_{12} = \frac{\sum_{i=1}^{N} e_i^4}{\sqrt{\sum_{i=1}^{N} e_i^2}}$
Mean of absolute value	$RE_5 = \frac{1}{N}\sum_{j=1}^{N}\lvert e_i\rvert$	Pulse factor	$RE_{13} = \frac{\max(e_i)-\min(e_i)}{\frac{1}{N}\sum_{j=1}^{N}\lvert e_i\rvert}$
Standard deviation	$RE_6 = \sigma = \sqrt{\frac{\sum_{j=1}^{N}(e_i-\bar{e}_i)}{N}}$	Margin factor	$RE_{14} = \frac{\max(e_i)-\min(e_i)}{\left[\frac{1}{N}\sum_{j=1}^{N}\lvert e_i\rvert\right]^2}$
Skewness	$RE_7 = \sqrt{\frac{1}{6N}\sum_{j=1}^{N}\left(\frac{e_i-\mu}{\sigma}\right)^3}$	Upper control limit	$RE_{15} = UCL = \mu + 3\frac{\sigma}{\sqrt{n}}$
Kurtosis	$RE_8 = \sqrt{\frac{N}{24}\left[\frac{1}{N}\sum_{j=1}^{N} -3\right]}$	Lower control limit	$RE_{16} = LCL = \mu - 3\frac{\sigma}{\sqrt{n}}$

3 Case Study

3.1 Benchmark for Calibration of the Proposed Concept

A three-story frame aluminum structure found in the literature [23] was selected as a benchmark to demonstrate the effectiveness of the proposed concept. As shown in Fig. 2(a), the structure consists of an electro-dynamic shaker mounted to the base for excitation, and the extra plate at top of the 3rd floor separated by columns to form an adjustable gap (Fig. 2(b)). Noted that the contact of the bumper and column result in non-linearity to simulate the cases in actual situation, where structures could experience the crack opening and closing or loose of bolt connection. Four sensors (accelerators), as marked by Sensors 1 to 4 in Fig. 2(a), were installed at the floors to capture the dynamic response during the excitation.

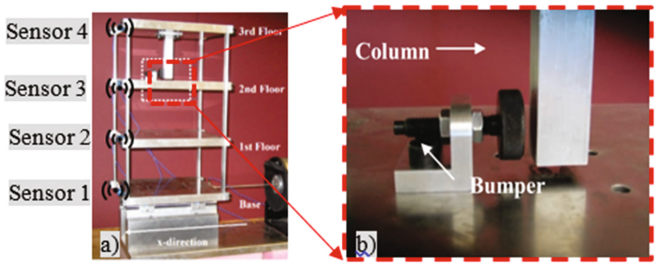

Fig. 2. Three-story frame structure [23]: (a) overview and test setup and (b) adjustable bumper and column

3.2 Scenarios Designed for Data-Driven Structural Diagnosis

Table 2 shows the designed 17 different scenarios, as documented in the literature. Each scenarios has 10 times testing and each floor has been installed with an acceleration sensor. The parameters AR and RE have been selected as damage features.

Table 2. Test matrix of the structural state conditions [12]

Label	State condition	Description
Undamaged states (# 1 to 9)		
State#1	Undamaged	Baseline condition
State#2	Undamaged	Added mass (1.2 kg) at the base
State#3	Undamaged	Added mass (1.2 kg) on the 1st floor
State#4	Undamaged	States 4–9: 87.5% stiffness reduction at various position to stimulate temperature impact (more detail in the reference)
State#5	Undamaged	
State#6	Undamaged	
State#7	Undamaged	
State#8	Undamaged	
State#9	Undamaged	
Damaged states (# 10 to 17)		
State#10	Damaged	Gap (0.20 mm)
State#11	Damaged	Gap (0.15 mm)
State#12	Damaged	Gap (0.13 mm)
State#13	Damaged	Gap (0.10 mm)
State#14	Damaged	Gap (0.05 mm)
State#15	Damaged	Gap (0.20 mm) and mass (1.2 kg) at the base
State#16	Damaged	Gap (0.20 mm) and mass (1.2 kg) on the 1st floor
State#17	Damaged	Gap (0.20 mm) and mass (1.2 kg) on the 1st floor

4 Results and Discussions

4.1 Effectiveness of Various Feature Extraction Methods and Sensitivity

As stated in the case study, the nonlinear damage was induced by the impact of the bumper and column (see Fig. 2(b)) at the the 2nd and 3rd floors near Sensors 3 and 4, as schematically shown in Fig. 3. These three feature extraction techniques, AR, VAR, SVD and their residuals (RE), exhibit the different levels of the effectiveness for pattern recognition. As shows in Fig. 3, the statistical analysis of dynamic response at each floor through sensors were displayed using the SVD feature extraction, where the blue lines mean the undamaged states (Cases 1–9) and the pink lines represent the damaged states (Case 10–17). For each state, residual has been selected with 1000 times steps, as shown in the x axis. Two dash lines in red shown in Fig. 3 are the maximum and minimum residual values from undamaged state, respectively. Clearly, all of the residual plots are on the same scale for the undamaged states, while it is apparent that all damaged states exhibit much higher response for all sensors.

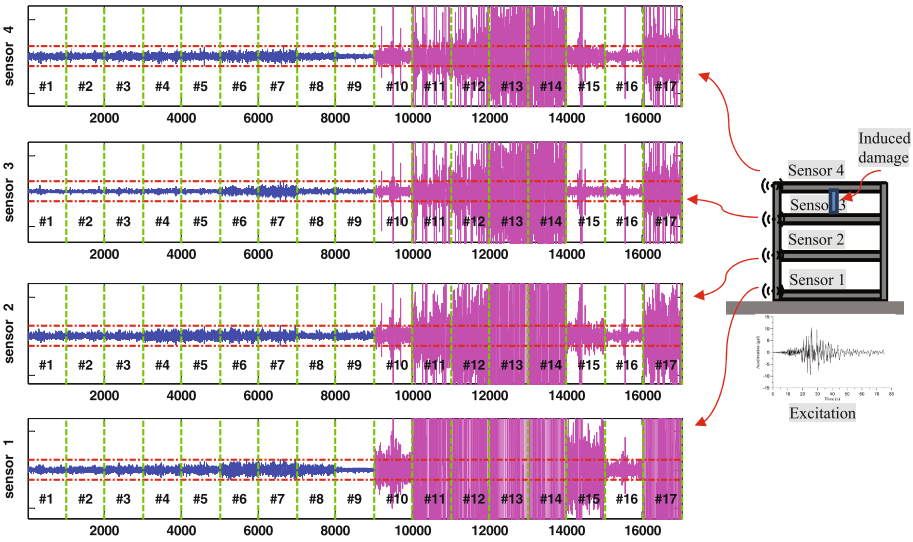

Fig. 3. Residuals from SVD for each state (undamaged state 1–9, damaged state 10–17)

Moreover, each residual of damaged state exhibits some singularities, which was responsible for the impact of the column and the bumper, and the time domain residual method can capture each individual impact. Also, Fig. 3 shows that the SVD method has the high sensitivity to allow identifying conditions between damage and undamaged states, even for data from Sensor 1, which is far away from the damage resources.

Figure 4 was plotted to demonstrate the effectiveness of each feature extraction approach. Clearly, the AR model could effectively identify the presence of damage conditions (Cases 10–17) using data from Sensor 3, but apparently such capability

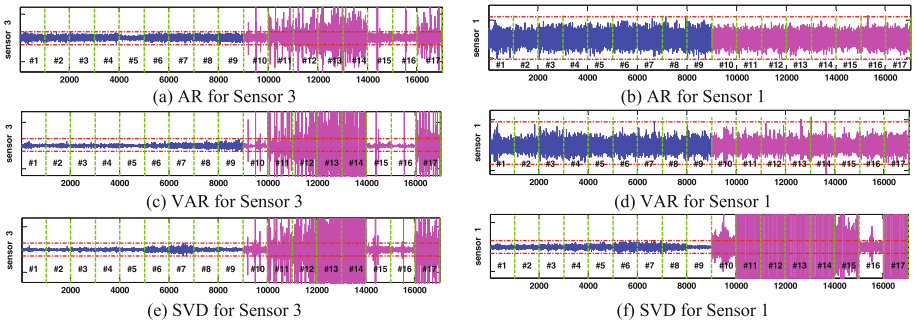

Fig. 4. Residuals from three techniques for each state at Sensors 1 and 3 (undamaged state 1–9, damaged state 10–17)

diminishes when processing data from Sensor 1 (or 2). Furthermore, although the VAR residual shows a few difference between damage and undamaged states for Sensor 1, such identification could not be valid if there are more interference. Differently, the SVD method exhibits much higher sensitive to damage as compared to other two approaches. It is mainly because the SVD uses the block Hankel matrix (see Eq. (13)), where information of all sensors are captured and in turn, enhance the sensitivity. It should be noted that since there are singularities in the cases for damage states, the SVD could demand much longer computation time than other two methods.

4.2 Damage Detection and Their Effectiveness

The residual of probability of designed states, including state 1 (original undamaged state) and state 10 (0.2-mm gap), are plotted in Fig. 5. The probability plot is a method to evaluate the data which is fit for some distribution. We assume the residual fits the Normal distribution. The probability is generated from an estimated cumulative distribution function (CDF) from the sample, and then scales are used to make the ideal distribution to a straight line. As clearly illustrated in Fig. 5, each method residuals (AR, VAR or SVD) of original state (state 1) shows a good fit for normal distribution. A good distribution fit is one where the observation is near the fitted dash line. Differently, in the context of damaged states (see state 10), probability curves are not straight line anymore, as shown in Fig. 5, that it is, there are some abnormal points from the normal distribution due to damages. Hence, the estimated CDF could aid to

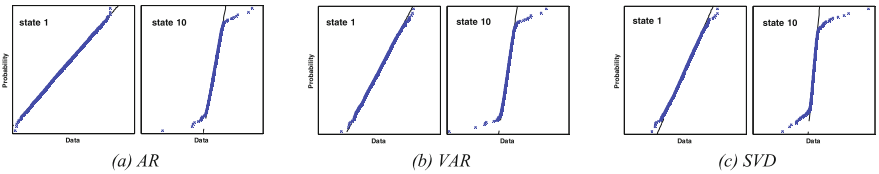

Fig. 5. Normal probability distribution of residual for three features at sensor 4

identify potentially early damages. The comparison of three approaches also confirmed that the SVD residuals have more sensitivity to damage, as identified in Fig. 4.

The SVM maps the feature space to a nonlinear space to get a better pattern recognition. In this study, 50 experiments data have been selected for each state, the total sample is 850. The samples have been separate as training group and testing group with equal number. Figure 6 plots the receiver operating characteristic (ROC) curves for three features and their associated residuals for the accomplishment of the machine learning. Clearly, the ROC curves showed that all features identified in this study has an almost perfect discrimination ability, even with different operational and environmental states.

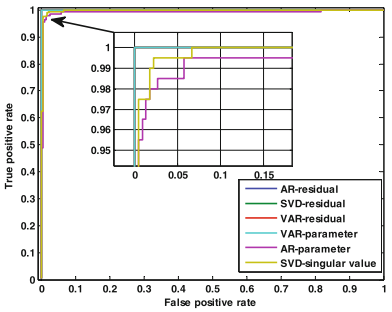

Fig. 6. The ROC curves of different feature extraction method

5 Conclusions

This study presented new data-driven structural diagnosis and damage detection with three feature extraction techniques for facilitating the pattern recognition and improving the identification between damaged and undamaged cases. Results have demonstrated the SVD model has significantly higher accuracy and sensitivity as compared to other two approaches, as it has higher sensitivity to the local fluctuation. Furthermore, the probability curves of three feature extraction approaches further confirm that the damaged states behave nonlinear as compared to original undamaged ones, and thus lead to a higher reliable data identification.

Acknowledgments. The authors gratefully acknowledge the financial support provided by Ozbun Economic Development Award, National Natural Science Foundation of China (No. 51468023), ND Department of Commerce, US DOT and US DOT CAAP Pipeline and Hazardous Materials.

References

1. Zou, Y., Tong, L., Steven, G.P.: Vibration-based model-dependent damage (delamination) identification and health monitoring for composite structures: a review. J. Sound Vib. **230**, 357–378 (2000)

2. Kopsaftopoulos, F.P., Fassois, S.D.: A functional model based statistical time series method for vibration based damage detection, localization, and magnitude estimation. Mech. Syst. Signal Process. **39**, 143–161 (2013)
3. Magalhães, F., Cunha, A., Caetano, E.: Vibration based structural health monitoring of an arch bridge: from automated OMA to damage detection. Mech. Syst. Signal Process. **28**, 212–228 (2012)
4. Masciotta, M.G., Ramos, L.F., Lourenço, P.B., Vasta, M.: Damage detection on the Z24 bridge by a spectral-based dynamic identification technique. In: Dynamics of Civil Structures, vol. 4, pp. 197–206. Springer, Berlin (2014)
5. Comanducci, G., Magalhães, F., Ubertini, F., Cunha, Á.: On vibration-based damage detection by multivariate statistical techniques: application to a long-span arch bridge. Struct. Health Monit. **15**(5), 505–524 (2016)
6. Ge, R., Pan, H., Lin, Z., Gong, N., Wang, J.: RF-powered battery-less wireless sensor network. In: 5th International Symposium on Next-Generation Electronics Hsinchu, Taiwan (2016)
7. Lin, Z., Yan, F., Azimi, M., Azarmi, F., Al-Kaseasbeh, Q.: A revisit of fatigue performance based welding quality criteria in bridge welding provisions and guidelines. In: International Industrial Informatics and Computer Engineering Conference (IIICEC), Shaanxi, China (2015)
8. Gerist, S., Maheri, M.R.: Multi-stage approach for structural damage detection problem using basis pursuit and particle swarm optimization. J. Sound Vib. **384**, 210–226 (2016)
9. Jang, J.: Development of Data Analytics and Modeling Tools for Civil Infrastructure Condition Monitoring Applications. Columbia University, Columbia (2016)
10. Ko, J.M., Ni, Y.Q.: Technology developments in structural health monitoring of large-scale bridges. Eng. Struct. **27**, 1715–1725 (2005)
11. Rashedi, R., Hegazy, T.: Capital renewal optimisation for large-scale infrastructure networks: genetic algorithms versus advanced mathematical tools. Struct. Infrastruct. Eng. **11**, 253–262 (2015)
12. Gui, G., Pan, H., Lin, Z., Li, Y., Yuan, Z.: Data-driven support vector machine with optimization techniques for structural health monitoring and damage detection. KSCE J. Civil Eng. **21**(2), 523–534 (2016)
13. Pan, H., Ge, R., Wang, J., Gong, N., Lin, Z.: Integrated wireless sensor networks with uas for damage detection and monitoring of bridges and other large-scale critical civil infrastructures. In: NDE/NDT for Highway and Bridges: Structural Materials Technology, Portland, OR, USA (2016)
14. Yan, F., Chen, W., Lin, Z.: Prediction of fatigue life of welded details in cable-stayed orthotropic steel deck bridges. Eng. Struct. **127**, 344–358 (2016)
15. Widodo, A., Yang, B.-S.: Application of nonlinear feature extraction and support vector machines for fault diagnosis of induction motors. Expert Syst. Appl. **33**, 241–250 (2007)
16. Gersch, W.: Estimation of the autoregressive parameters of a mixed autoregressive moving-average time series. IEEE Trans. Autom. Control **15**, 583–588 (1970)
17. Yao, R., Pakzad, S.N.: Autoregressive statistical pattern recognition algorithms for damage detection in civil structures. Mech. Syst. Signal Process. **31**, 355–368 (2012)
18. Figueiredo, E., Figueiras, J., Park, G., Farrar, C.R., Worden, K.: Influence of the autoregressive model order on damage detection. Comput. Aided Civil Infrastruct. Eng. **26**, 225–238 (2011)
19. Zivot, E., Wang, J.: Modeling Financial Time Series with S-PLUS®. Vector autoregressive models for multivariate time series, pp. 385–429. Springer, New York (2006)
20. Ouali, M.A., Chafaa, K.: SVD-based method for ECG denoising. In: 2013 International Conference on Computer Applications Technology (ICCAT), pp. 1–4 (2013)

21. Sharma, A., Amarnath, M., Kankar, P.: Feature extraction and fault severity classification in ball bearings. J. Vib. Control **22**, 176–192 (2016)
22. Boldt, F.D.A., Rauber, T.W., Varejao, F.M.: Feature extraction and selection for automatic fault diagnosis of rotating machinery
23. Figueiredo, E., Park, G., Figueiras, J., Farrar, C., Worden, K.: Structural Health Monitoring Algorithm Comparisons Using Standard Data Sets, Report (2009)
24. Suykens, J.A.K., Vandewalle, J.: Least squares support vector machine classifiers. Neural Process. Lett. **9**, 293–300 (1999)
25. Furey, T.S., Cristianini, N., Duffy, N., Bednarski, D.W., Schummer, M., Haussler, D.: Support vector machine classification and validation of cancer tissue samples using microarray expression data. Bioinformatics **16**, 906–914 (2000)